






# Novel bacteriophages targeting wheat phyllosphere bacteria carry DNA modifications and single-strand breaks

Peter Erdmann Dougherty<sup>a</sup> , Maja Schmidt Pedersen<sup>a</sup>, Laura Milena Forero-Junco<sup>a</sup>,  
Alexander Byth Carstens<sup>a</sup>, Jos M. Raaijmakers<sup>b</sup>, Leise Riber<sup>a,\*</sup> , Lars Hestbjerg Hansen<sup>a,\*</sup> 

<sup>a</sup> Department of Plant and Environmental Science, University of Copenhagen, Frederiksberg, Denmark

<sup>b</sup> Department of Microbial Ecology, Netherlands Institute of Ecology (NIOO-KNAW), Wageningen, the Netherlands

## ARTICLE INFO

### Keywords:

Bacteriophages  
Genomics  
DNA modifications  
Phyllosphere

## ABSTRACT

The phyllosphere microbiome can positively or negatively impact plant health and growth, but we currently lack the tools to control microbiome composition. Contributing to a growing collection of bacteriophages (phages) targeting bacteria living in the wheat phyllosphere, we here isolate and sequence eight novel phages targeting common phyllosphere *Erwinia* and *Pseudomonas* strains, including two jumbo phages. We characterize genomic, phylogenetic, and morphological traits from these phages and argue for establishing four novel viral genera. We also search the genomes for anti-defense systems and investigate DNA modifications using Nanopore sequencing. In *Pseudomonas* phage Rembedalseter we find evidence of 13 motif-associated single-stranded DNA breaks. A bioinformatics search revealed that 60 related *Pseudomonas* phages are enriched in the same motif, suggesting these single-stranded nicks may be widely distributed in this family of phages. Finally, we also search the Sequence Read Archive for similar phages in public metagenomes. We find close hits to the *Erwinia* jumbo-phage Kaldavass in a wide variety of plant, food, and wastewater metagenomes including a near-perfect hit from a Spanish spinach sample, illustrating how interconnected geographically distant phages can be.

## 1. Introduction

Although Earth's surface is mostly ocean, the land surface area is dominated by plants, with vegetation covering 69% of the land surface area (Li et al., 2023). This extensive aerial vegetation is in turn colonized by bacteria, fungi, viruses, and other microorganisms that collectively constitute the phyllosphere microbiome (Sohrabi et al., 2023). The host plant often benefits from this microbial community through growth promotion (Herpell et al., 2023) or enhanced stress tolerance (Liu et al., 2023), but the phyllosphere is also a major niche for plant pathogens (Pfeilmeier et al., 2016). For this reason, techniques capable of manipulating the phyllosphere microbiome are of great interest.

One such potential tool are bacteriophages (phages); viruses that infect bacteria (Clokiet al., 2011). Phages have attracted significant interest as tools for microbiome manipulation, either for the direct elimination of target bacteria (phage therapy/biocontrol) (Frampton et al., 2012), or through more indirect, broad-scale microbiome shifts (virome transplants) (Rasmussen et al., 2020). Broadly speaking, phage lifestyles can be split into two main types; virulent phages, which

replicate immediately upon entering a viable host cell and kill the host soon after, and temperate phages, which can enter a dormancy state (prophage) within the host cell, retaining the ability to undergo induction and kill the host later (Howard-Varona et al., 2017). Virulent phages are usually preferred for microbiome manipulation as temperate phages may integrate into new hosts, spreading phage resistance and possible virulence factors (Frampton et al., 2012).

To defend against bacteriophages, bacteria have evolved a tremendously diverse array of defense systems (Georjon and Bernheim, 2023) and in response, phages have evolved counter-defense systems (Duan et al., 2024). One avenue of counter-defense is DNA modification, where phages add chemical groups to the canonical nucleotides and thus avoid recognition by some defense systems (Weigele and Raleigh, 2016b). Although most modifications are undetectable with common DNA sequencing platforms (such as Illumina), their presence may be detected by sequencing non-amplified DNA on platforms such as PacBio or Oxford Nanopore Technologies (ONT) (Nielsen et al., 2023). Recently, this approach was applied to human gut viromes, where an astonishing 97.6% of phages exhibited methylation (Sun et al., 2023). However,

\* Corresponding authors.

E-mail addresses: [lriber@plen.ku.dk](mailto:lriber@plen.ku.dk) (L. Riber), [lhha@plen.ku.dk](mailto:lhha@plen.ku.dk) (L.H. Hansen).

<https://doi.org/10.1016/j.virusres.2024.199524>

Received 28 October 2024; Received in revised form 24 December 2024; Accepted 29 December 2024

0168-1702/© 2025 The Authors. Published by Elsevier B.V. This is an open access article under the CC BY license (<http://creativecommons.org/licenses/by/4.0/>).

more complex modifications may not be detectable in metagenomes, and screening for DNA modifications is not commonly performed for phage isolates (or viromes). We therefore know little about the distribution and frequency of phage DNA modifications in different environments.

In the phyllosphere, phages are highly diverse (Dougherty et al., 2023; Forero-Junco et al., 2022) and have been shown to significantly alter bacterial abundances (Morella et al., 2018). Recently, we also showed that some wheat phyllosphere bacteria harbor spontaneously induced prophages capable of killing rival bacterial strains, thus facilitating intra-species warfare (Dougherty et al., 2023). Although using prophage-infected bacteria to manipulate the phyllosphere microbiome is an intriguing idea, it does risk unwanted horizontal gene transfer. Approaching the problem from another angle, we have therefore previously isolated and characterized virulent phages against *Sphingomonas* strains from the same wheat phyllosphere as a first step in establishing a collection of phages targeting wheat phyllosphere bacteria (Riber et al., 2023). Here, we continue this effort, isolating eight phages against wheat phyllosphere bacteria from two common phyllosphere genera, *Erwinia* and *Pseudomonas*. Sequencing revealed these phages to be highly diverse, with phylogenetic analysis supporting the establishment of four novel phage genera. We also conducted a bioinformatic search for anti-defense systems and investigated DNA structure and modifications in the phage genomes using ONT sequencing, identifying two methylated phage genomes, two phages with probable hyper-modifications, and one phage with single-stranded coverage indicative of motif-associated single-stranded DNA breaks (nicks). We find that a conserved group of *Pseudomonas* phages is enriched in the same nick-associated motif, and we investigate the distribution of this motif throughout their genomes.

## 2. Materials and methods

### 2.1. Phage isolation and enrichment

The phages were isolated from household organic waste from a waste-management company (HCS A/S, Glostrup, Denmark). We have previously found organic waste to be a rich source for phages targeting plant-associated bacteria (Alanin et al., 2023; Djurhuus et al., 2020; Jorgensen et al., 2020; Riber et al., 2023). Following this established protocol, we centrifuged the organic waste samples at 5000 x g for 10 min followed by filtering with a 0.45 µm PVDF syringe filter (Merck Millipore, Germany). Seven *Erwinia* and *Pseudomonas* strains previously isolated from the wheat phyllosphere were used as bacterial hosts (Dougherty et al., 2023). 100 µL of organic waste supernatant was added to 100 µL of the overnight bacterial cultures and plated with a double agar overlay with 4 mL LB soft agar (0.45% agarose, supplemented with 10 mM CaCl<sub>2</sub> and MgCl<sub>2</sub>) on top of LB agar. After overnight incubation at 28 °C, plaques were picked, resuspended in SM buffer (100 mM NaCl, 10 mM MgSO<sub>4</sub>, 50 mM Tris-HCl, pH 7.5), and filtered using 0.22 µm syringe filters. To purify each phage isolate, plaques were picked and replated three times for each phage isolate.

High-titre (>10<sup>8</sup> plaque forming units /mL) phage enrichments were made by adding low titres of purified phage stock to exponential cultures of respective bacterial hosts in liquid LB media. The cultures were incubated overnight with shaking (225 rpm) at 28 °C, followed by centrifugation at 8000 x g for 5 min to pellet the bacteria. The supernatants were then filter-sterilized as before.

### 2.2. TEM microscopy

To prepare phage samples for transmission electron microscopy (TEM) imaging, high-titre phage enrichments were purified by cesium-chloride (CsCl) gradient ultracentrifugation using an Optima XE-90 ultracentrifuge (Beckman Coulter, USA) with three CsCl density layers (1.3, 1.45, and 1.7 g/cm<sup>3</sup>). At the Electron Microscopy Facility at the

University of Leicester, 5 µL of purified phage samples were spotted to a freshly glow-discharged carbon film grid for 2 min, washed with deionized water, and negatively stained with 1% uranyl acetate. Samples were then viewed on a JEM-1400 TEM (JEOL, Japan) with an accelerating voltage of 120 kV, with images taken using a Xarosa digital camera RADIUS software (EMSIS, Germany). Length and width values are the average of five measurements, shown with standard deviation.

### 2.3. DNA isolation and sequencing

DNA isolation was performed as in prior work (Dougherty et al., 2023). Briefly, starting with high-titre phage enrichments, DNase I (25 units/mL) and RNase A (25 µg/mL) (A&A Biotechnology, Poland) were added to 500 µL of each phage amplification, and incubated for an hour at 37 °C. The nucleases were deactivated and encapsulated phage DNA released by incubation with EDTA (50 µM), SDS (0.1 %), and Proteinase K (1 mg/mL) at 55 °C for an hour. Proteinase K was deactivated by incubation at 70 °C for 10 min. The raw DNA extractions were then purified with the Clean and Concentrator-5 kit (Zymo Research, USA). A Qubit 2.0 fluorometer with a High Sensitivity dsDNA assay (ThermoFisher, USA) was used to quantify the DNA concentrations. Illumina sequencing libraries were built using the NEBNext Ultra II FS DNA Library Prep kit (New England Biolabs, USA) according to the manufacturer's protocol. Libraries were sequenced on a 151-bp paired-end sequencing run with the Illumina iSeq platform (Illumina, San Diego, USA).

To detect potential DNA modifications, the phage DNA was sequenced using the Oxford Nanopore Technologies (ONT) platform as previously described (Kot et al., 2020). Briefly, a whole genome amplification (WGA) of each phage DNA isolation was prepared according to protocol using the illustra Ready-To-Go GenomePhi V3 DNA amplification kit (GE Healthcare, USA), followed by debranching with S1 nuclease (ThermoFisher Scientific, USA). The product was then purified using the DNA Clean and Concentrator-5 kit (Zymo Research, USA). These amplified copies of the original DNA isolations contain no DNA modifications, and hence were used as a negative control.

Barcoded ONT libraries were built from each raw phage DNA isolation and WGA copy using the Rapid Barcoding Kit 96 RBK 110-96 (ONT, UK). The libraries were then sequenced together on the MinION platform using an R9 flowcell and MinKNOW.

### 2.4. Genomic characterization of nicked phages

To assemble the isolated phage genomes, Illumina reads were trimmed and quality-controlled using TrimGalore (v0.6.6) (Felix Krueger, 2021) and assembled with SPAdes (3.13.1) (Bankevich et al., 2012). As in previous work (Riber et al., 2023), assemblies were manually quality-controlled and reoriented with respect to their correct start sites in CLC Genomics Workbench (v22). Phage genomes were annotated using Pharokka (v1.4.1) (Bouras et al., 2023). Similar phages were found using a combination of whole-genome BLASTN and tBLASTx searches (2.14.1+) against the INPHARED database (August 2023) (Cook et al., 2021). In the case of *Pseudomonas* phage Rembedalsseter, a BLASTN search (webserver, October 2023) was also conducted to identify similar sequences in bacterial assemblies. Genomad (v1.7.0) (Camargo et al., 2024) was used to predict prophages in the bacterial assemblies with the best BLASTN hits, and the relevant prophage regions extracted.

For each phage isolate, selections of the top BLAST hits were made for further analysis. In each case, the top five BLASTN hits (ranked by score) were included in addition to a manual selection of other related phages. To quantify the intergenomic similarity between related phages, pairwise whole-genome nucleotide identities were calculated and visualized using VIRIDIC (webserver) (Moraru et al., 2020), and the recommended 70% genome identity cutoff from VIRIDIC was used to classify phages at the genus level (Moraru et al., 2020; Turner et al.,

2021). Selected related phages were also visualized using clinker (v0.0.28) (Gilchrist and Chooi, 2021) to show amino acid alignments between phage coding sequences. BACPHLIP (v0.9.6) (Hockenberry and Wilke, 2021) was also used to predict the lifestyle (virulent/temperate) of each phage isolate. Phages with a virulent score > 0.5 were classified as virulent.

Using the Pharokka annotations, large terminase subunit (TerL) proteins were also identified, and a BLASTP (2.14.1+) search was conducted to identify the closest hits. Muscle (v3.8.1551) (Edgar, 2004) was used to align the TerL amino acid sequences, and IQTREE (v2.2.5) (Minh et al., 2020) was used to generate nonparametrically bootstrapped (n=1000) phylogenetic maximum likelihood trees of the closest five BLASTP hits (ranked by score) along with a manual selection of other related phages. The trees were then visualized with ITOL v6 (Letunic and Bork, 2021) and rooted at midpoint.

## 2.5. Environmental distribution of similar phages

To summarize the environments in which similar phages are found, we combined metadata from three sources; genus-level (70% nucleotide identity) phage isolates, genus-level metagenomically assembled contigs from the IMG/VR v4 database, and Sequence Read Archives (SRA) from metagenomic samples. Using Sourmash Branchwater (Luiz Irber, 2022) to search for similar phages in >1,000,000 metagenomic SRAs, we reported SRAs which contain > 70% of the sampled phage 21-mers. We then combined the environmental metadata from these three sources to form a profile for each phage. We also downloaded reads from a single SRA (SRR14611561) with 100% containment to phage Kaldavass and mapped them to the Kaldavass genome using bwa-mem (Li and Durbin, 2009) to verify read coverage.

## 2.6. Analysis of anti-defense systems and DNA modifications

The dbAPIS database consists of experimentally verified anti-defense proteins together with bioinformatically-derived protein families (Yan et al., 2023). Using the derived protein families, we conducted an HMM search for similar proteins in the phage genomes, recording hits with an e-value < 0.05. For each hit, we subsequently conducted a BLASTP against the experimentally verified protein in each family.

To detect phage genome nucleotide modifications in the Nanopore sequencing data, we used the TOMBO\_HP workflow (Junco, 2024). In brief, raw sequencing signals were basecalled using Guppy 6.3.9 with the high-accuracy model 'dna\_r9.4.1\_450bps\_sup.cfn'. The basecalled reads were aligned to the phage genomes using minimap2 (v2.24) (Li, 2018). Then, the raw signal from the mapped reads was anchored to the reference genome (resquigged) using Tombo (1.5.1). This software was used to detect modifications, by comparing the signal from the native DNA to that of the control sample that underwent Whole Genome Amplification (WGA). The modified fraction (modfrac) statistics from Tombo were used to generate plots and tables that were manually inspected to detect the DNA modification motifs. Known motifs associated with Dam and Dcm methylation were further examined with Tombo using motif-specific models available for *Escherichia coli* Dam and Dcm methylation to confirm the presence of these specific methylation events.

For the motif analysis of *Pseudomonas* phage Rembedalsseter, the 250 closest phage genomes were selected by tBLASTx search against the INPHARED database (August 2023), ranked by aggregated score per genome. Distances between all genome pairs were calculated using the weighted gene repertoire relatedness (wGRR) (Pfeifer et al., 2021). Occurrences of the motif WACTRTGAC were located in each genome using seqkit v2.5.1 (Shen et al., 2016). Pharokka was used to gene-call the 60 closest genomes and reorientate them relative to the conserved *terL* gene. Motif positions were then calculated relative to genome length and coding sequences.

## 3. Results and discussion

Eight phages were isolated from organic waste samples using seven bacterial strains previously isolated from the wheat phyllosphere (Dougherty et al., 2023) as replication hosts: four *E. aphidicola* strains, two *P. poae* strains, and one *P. trivialis* strain (Table 1). Host genome assemblies available under NCBI BioProject PRJNA951732.

The isolated phages were diverse in terms of genome and GC content, with sizes ranging from 45,228 bp to 366,556 bp and GC content between 38.4% - 56.9%. Using BACPHLIP to predict lifestyle, all phages were predicted to be virulent.

### 3.1. *Erwinia* phages Vettismorki and Gravdalen

The two closely related *Erwinia* phages Vettismorki and Gravdalen were isolated against the *E. aphidicola* strains B01\_5 and N2\_6, respectively.

TEM imaging showed *Erwinia* phages Vettismorki and Gravdalen to be tailed, contractile phages. Vettismorki had a tail length of 119±4 nm, head length of 121±4 nm, and head width of 90±2 nm, while Gravdalen had a tail length of 117±2 nm, head length of 119±4 nm, and head width of 85±3 nm. Both phages also have long tail fibers (shown for Gravdalen in Fig. 1B). Vettismorki and Gravdalen are very similar genetically (93.5% nucleotide similarity), with genome sizes of 171,806 bp and 171,558 bp and GC contents of 38.62% and 38.66%, respectively.

Phylogenetically, *Erwinia* phages Vettismorki and Gravdalen are closest to *Serratia* phages X20 and Chi14 (Chen et al., 2017) and *Erwinia* phage Virsatis27, both with respect to whole genome nucleotide identity and the TerL maximum likelihood tree (Fig. 1C-D). All three of these phages are classified within the genus *Winklervirus*, therefore also placing Vettismorki and Gravdalen within *Winklervirus*. Vettismorki is so closely related to X20 (96.3% nucleotide similarity) that it should be placed in the same species; *Winklervirus* xtventy. The genus *Winklervirus* lies within the subfamily *Tevenvirinae*, named for the representative species *Escherichia* phage T4, and Vettismorki and Gravdalen are shown to be related to T4 (Fig. 1C-E).

### 3.2. *Erwinia* phages Hallingskeid and Kaldavass

*Erwinia* phages Hallingskeid and Kaldavass were isolated against *E. aphidicola* strains B01\_10 and W09\_2, respectively.

TEM imaging showed both phages are large phages with contractile tails. Hallingskeid had a tail length of 131±4 nm, head length of 136±3 nm, and head width of 111±8 nm, while Kaldavass had a tail length of 128±5 nm, head length of 131±3 nm, and head width of 112±6 nm. Both phages also have short tail fibers terminating in rounded appendages almost resembling small feet. Related jumbo phages (*Pectobacterium* phage CBB, *Klebsiella* phage Rak2) are known to encode complex tail fiber assemblies (Buttimer et al., 2017; Simoliunas et al., 2013) and these feet-like appendages may be analogous complexes. Interestingly, both Hallingskeid and Kaldavass have multiple proteins annotated as tail fibers (two and six proteins, respectively), further supporting this interpretation.

Sequencing showed that the large capsids of the viral particles were reflected in genome size; Hallingskeid and Kaldavass were 366,158 bp and 366,556 bp respectively, far above the 200 kbp cutoff for jumbo phages. Although the two phages are of similar size and morphology, they share little nucleotide identity (26.3% whole-genome similarity). They are also related to other Enterobacterial jumbo phages of similar sizes (Fig. 2C). In particular, Kaldavass is similar to *Xanthomonas* phage Xbc2 (Villicaña et al., 2024) (84.6% similarity) with related TerL proteins (DMFGBAK\_CDS\_0386 and XGIBIPCR\_CDS\_0379) (Fig. 2D). Meanwhile, Hallingskeid is somewhat similar to *Escherichia* phage EJP2 (Jo et al., 2023) (39.5%) and has a more diverged TerL. Hence, Kaldavass should be placed in the genus *Mimavirus* with Xbc2, while



**Table 1**  
Overview of the 8 isolated phages, showing isolation host, genome length, GC content, and proposed genera. All phages are isolated from household organic waste from Glostrup, Denmark.

Name	Host	Length (bp)	GC (%)	Proposed genus	GenBank accession
Erwinia phage Vettismorki	<i>E. aphidicola</i> B01_5	171,806	38.6	<i>Winklervirus</i>	PQ464591
Erwinia phage Gravdalen	<i>E. aphidicola</i> N2_6	171,558	38.7	<i>Winklervirus</i>	PQ464594
Erwinia phage Hallingskeid	<i>E. aphidicola</i> B01_10	366,158	39.5	<i>Mimavirus</i>	PQ464590
Erwinia phage Kaldavass	<i>E. aphidicola</i> W09_2	366,556	38.4	Novel genus	PQ464595
Pseudomonas phage Rembedalsseter	<i>P. trivialis</i> B08_4	45,228	52.5	<i>Vicosavirus</i>	PQ464593
Pseudomonas phage Boevelstad	<i>P. poae</i> B04_10	92,884	44.9	Novel genus	PQ464592
Pseudomonas phage Torfinnsbu	<i>P. poae</i> Z9_5	53,022	56.9	Novel genus	PQ464596
Pseudomonas phage Milchi	<i>P. poae</i> Z9_5	174,859	45.5	Novel genus*	PQ464597

\* *Pseudomonas* phage Milchi should be placed into the same genus as *Pseudomonas* phage Astolliot, but this phage is currently misclassified within an incorrect genus (*Otagovirus*).

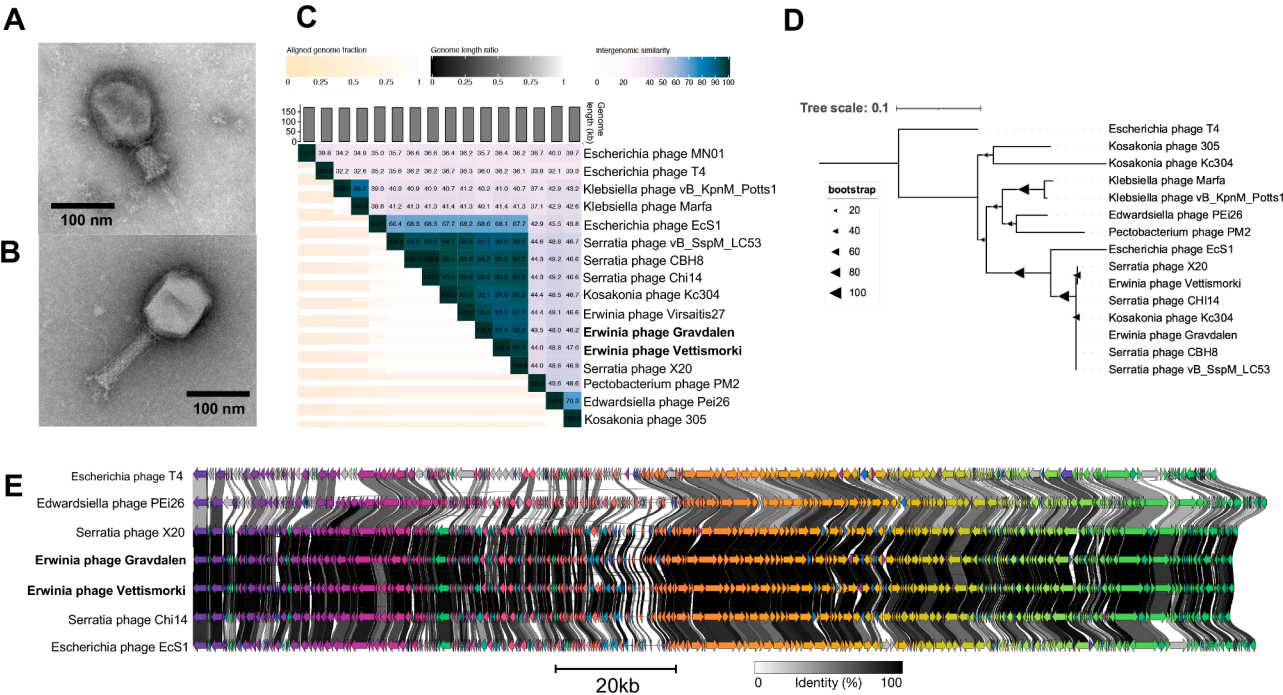


**Fig. 1.** Analysis of *Erwinia* phages Vettismorki and Gravdalen. (A) TEM imaging of *Erwinia* phage Vettismorki, tail contracted. (B) TEM imaging of *Erwinia* phage Gravdalen, tail non-contracted and tail fiber visible. (C) Whole-genome nucleotide similarity of Vettismorki and Gravdalen in comparison with select related phage genomes (VIRIDIC). (D) Bootstrapped maximum likelihood tree of large terminase subunit acid alignments with select related phages. (E) clinker figure showing amino-acid similarities between protein-coding sequences of select related phages. Protein clusters with > 30% sequence identity are coloured with the same colour.

Hallingskeid should form a novel genus. More broadly, all the aforementioned phages reside within the so-called group 2.2 jumbo phages which are distant descendants of the smaller *Tevenvirinae* phages (Iyer et al., 2021). Group 2.2 jumbo phages are distinct from the well-known Chimalliviridae, who encode a characteristic nuclear shell protein (Iyer et al., 2021; Prichard et al., 2023).

Although this group of phages diverge at the nucleotide level, aligning their proteins reveal a common architecture (Fig. 2E). Roughly, the genomes 150 kbp conserved region consisting primarily of well-annotated DNA/RNA metabolism and structural genes, flanked by variable 100 kbp regions on either side with many smaller genes of unknown functions.

3.3. *Pseudomonas* phage Rembedalsseter

*Pseudomonas* phage Rembedalsseter was isolated on the *P. trivialis* strain B08\_4.

TEM imaging shows this phage to have a symmetric icosahedral head (length and width 62±4 nm and 60±3 nm) and a tail length of 40±6 nm (Fig. 3A). Rembedalsseter’s genome reflects this modest size (45,228 bp)

and has a GC content of 52.5% (Table 1). The closest whole-genome hits to Rembedalsseter are *Pseudomonas* phages UFV-P2 (Eller et al., 2014) and NV1 (Storey et al., 2020) (76.7% and 69.5% whole-genome similarity respectively, Fig. 3B). TerL alignments also show these two phages to be Rembedalsseter’s closest neighbors (Fig. 3C). As both these phages reside within the genus *Vicosavirus*, Rembedalsseter should accordingly be placed within this genus. *Vicosavirus* is closely related to the genus *Bruynoghevirus*, which includes the well-studied *Pseudomonas* phage LUZ24 (Ceyssens et al., 2008). Members of both genera share considerable synteny (Fig. 3D), with bidirectionally transcribed DNA coding for early and middle genes on the left, and late genes on the right.

Interestingly, these *Vicosavirus* phages share considerable (>60%) whole-genome similarity) with a predicted prophage from bacterial strain *P. tolaasii* FP2293. In fact, UFV-P2’s TerL (YP\_006907045.1) is 100% identical to that of the *P. tolaasii* prophage, indicating a very close phylogenetic relationship. Similarly, the more-distantly related *Bruynoghevirus* PaP3 was shown to integrate within its bacterial host’s chromosome despite lacking any detectable integrase or transposase (Tan et al., 2007). However, phage lifestyle predictor BACPHLIP predicts all *Vicosavirus* and *Bruynoghevirus* members to be virulent, and no

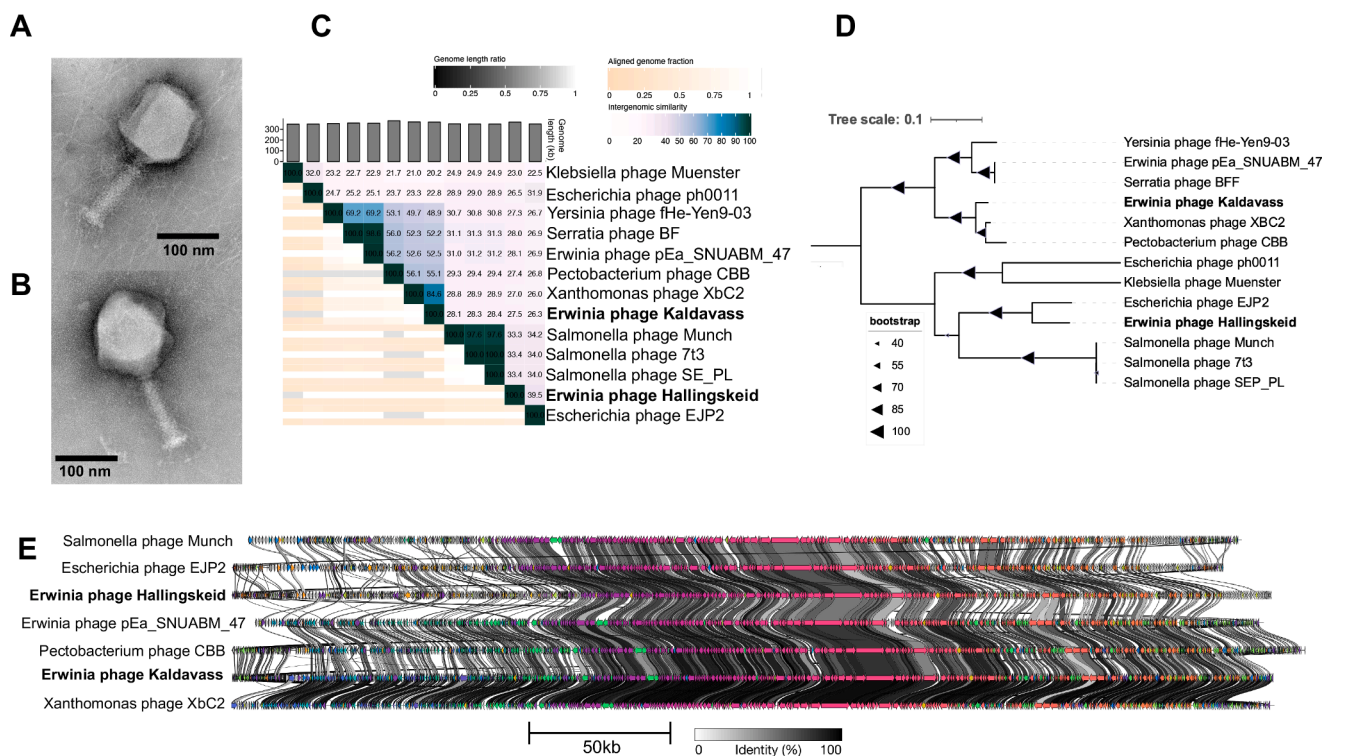


**Fig. 2.** Analysis of Erwinia phages Hallingskeid and Kaldavass. (A) TEM imaging of Erwinia phage Hallingskeid, with tail non-contracted and tail fibers visible. (B) TEM imaging of Erwinia phage Kaldavass, with tail non-contracted and tail fibers visible. (C) Whole-genome nucleotide similarity of Hallingskeid and Kaldavass in comparison with select related phage genomes (VIRIDIC). (D) Bootstrapped maximum likelihood tree of large terminase subunit amino acid alignments with select related phages. (E) clinker figure showing amino-acid similarities between protein-coding sequences. Protein clusters with > 30% sequence identity are coloured with the same colour.

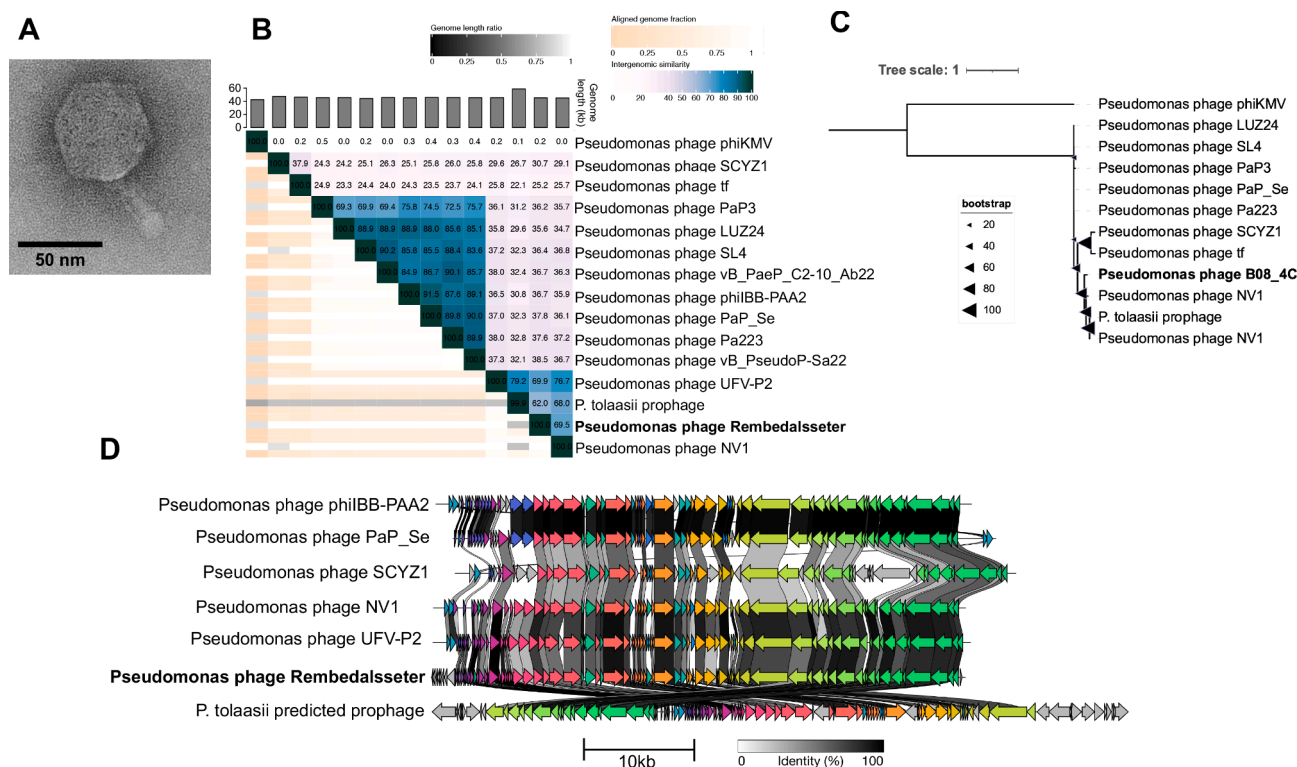


**Fig. 3.** Analysis of Pseudomonas phage Rembedalsseter. (A) TEM imaging of Pseudomonas phage Rembedalsseter. (B) Whole-genome nucleotide similarity of Rembedalsseter in comparison with select related phage genomes (VIRIDIC). (C) Bootstrapped maximum likelihood tree of large terminase subunit amino acid alignments with select related phages. (D) Clinker figure showing amino-acid similarities between protein-coding sequences. The *P. tolaasii* prophage prediction is in the same orientation as it appears in the bacterial genome. Protein clusters with > 30% sequence identity are coloured with the same colour.

integrases or transposases were found in any of the phages (including the *P. tolaasii* prophage) using Pharokka. At this point, it is unclear how PaP3 or the *P. tolaasii* prophage establish lysogeny, or whether the other *Vicosavirus* and *Bruynoghevirus* phages may have a temperate lifestyle (Knezevic et al., 2021).

### 3.4. *Pseudomonas* phage Boevelstad

*Pseudomonas* phage Boevelstad was isolated from plaques on host strain *P. poae* B04\_10.

*Pseudomonas* phage Boevelstad has a symmetrical icosahedral head (length and width  $74 \pm 3$  nm and  $72 \pm 2$  nm respectively),  $132 \pm 6$  nm contractile tail, and visible tail fibers (Fig. 4A). Although Boevelstad's tail is roughly the same size as those of jumbo phages Hallingskeid and Kaldavass, the head is much smaller, perhaps reflecting Boevelstad's smaller genome of 92,884 bp. Genetically, Boevelstad is quite distant from all NCBI phage genomes besides *Pseudomonas* phage PseuGes\_254, at 65.6% genome similarity (Fig. 4B). The TerL maximum likelihood tree also shows close relation to PseuGes\_254, which has not yet been placed in a named genus (Fig. 4C). However, Boevelstad is distinct enough to be placed in a new genus separate from PseuGes\_254.

Genome alignment also shows close relation between Boevelstad and PseuGes\_254, although there is also substantial alignment with other *Pseudomonas* phages such as phiK7A1 and M5.1 (Fig. 4D). Relative to the other phages shown in Fig. 4D, Boevelstad and PseuGes\_254 have a large inversion (bases 24,023 – 40,934 in Boevelstad). This genomic region codes for many proteins related to nucleotide metabolism, such as DNA primase/helicase (IPGPQISR\_CDS\_0074), DNA polymerase (IPGPQISR\_CDS\_0075), and ribonucleotide reductase (IPGPQISR\_CDS\_0090). Also of note is a predominantly non-protein-coding region (approx. 3.5 kbp, bases 66,796 – 70,162 in Boevelstad) present in all phages shown in Fig. 4D. This region is host to many tRNAs; in Boevelstad, 12 tRNAs are located here.

### 3.5. *Pseudomonas* phage Torfinnsbu

*Pseudomonas* phage Torfinnsbu was isolated on the bacterial strain

*P. poae* Z9\_5.

Morphologically, Torfinnsbu has a symmetric icosahedral head (length and width  $69 \pm 2$  nm and  $67 \pm 2$  nm respectively) and a long ( $159 \pm 8$  nm) flexible, striated, tail (Fig. 5A). Torfinnsbu has a 53,022 bp genome with a somewhat high GC content (56%). However, this is slightly below the GC content of the host strain *P. poae* Z9\_5 (60%) as is normal for phages (Simón et al., 2021).

Phylogenetically, however, Torfinnsbu does not have any close relatives among known phage isolates. *Pseudomonas* phage DDSR119 has 20% whole-genome nucleotide similarity to Torfinnsbu, but no other phage isolates have any substantial nucleotide similarity (Fig. 5B). Although the maximum likelihood tree (Fig. 5C) shows *Streptomyces* phage SF3's TerL (YP\_009213215.1) as the closest hit phylogenetically, the two phages otherwise share very few genes (Fig. 5D) and are therefore only very distantly related.

Whole-genome protein alignments (Fig. 5D) show Torfinnsbu shares homology with *Vibrio* phages vB\_VaM\_H2 and *Vibrio* phage NF over a leftmost region of ~22 kbp coding for structural genes. *Pseudomonas* phage DDSR119 also shares amino acid similarity with some of Torfinnsbu's structural genes, in addition to a downstream homologous region coding for DNA metabolism-associated proteins. Interestingly, one of Torfinnsbu's proteins is annotated as a ParB-like partition protein (RJUOAXPK\_CDS\_0074), which might indicate some type of plasmid-phage lifecycle. Although no other annotations were found that relate to plasmid functions, this protein is also conserved in DDSR119 (QMP23987.1).

### 3.6. *Pseudomonas* phage Milchi

*Pseudomonas* phage Milchi was also isolated on the *P. poae* strain Z9\_5.

*Pseudomonas* phage Milchi has a nearly symmetrical icosahedral head (length and width  $133 \pm 3$  nm and  $119 \pm 7$  nm) a  $129 \pm 5$  nm contractile, striated tail terminating in straight tail fibers (Fig. 6A). Milchi is a large phage with a genome length of 174,859 bp and encodes 29 predicted tRNAs.

Phylogenetically, Milchi is closely related to *Pseudomonas* phage

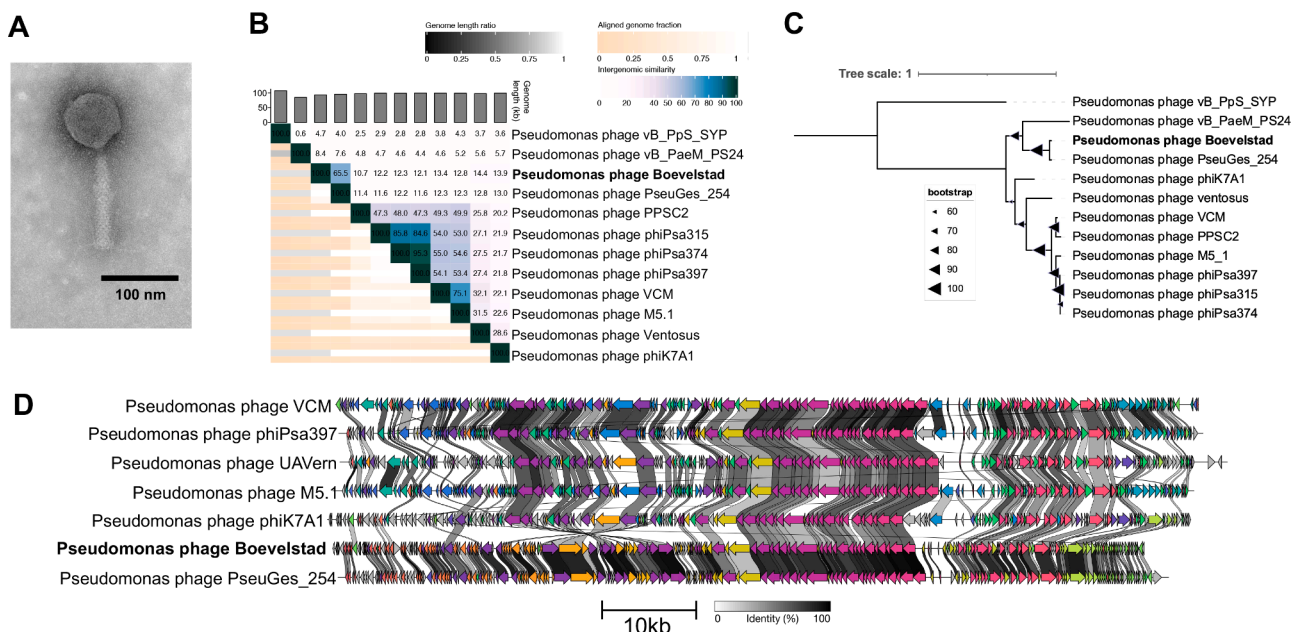


**Fig. 4.** Analysis of *Pseudomonas* phage Boevelstad. (A) TEM imaging of *Pseudomonas* phage Boevelstad. (B) Whole-genome nucleotide similarity of Boevelstad in comparison with select related phage genomes (VIRIDIC). (C) Bootstrapped maximum likelihood tree of large terminase subunit amino acid alignments with select related phages. (D) Clinker figure showing amino-acid similarities between protein-coding sequences. Protein clusters with > 30% sequence identity are coloured with the same colour.



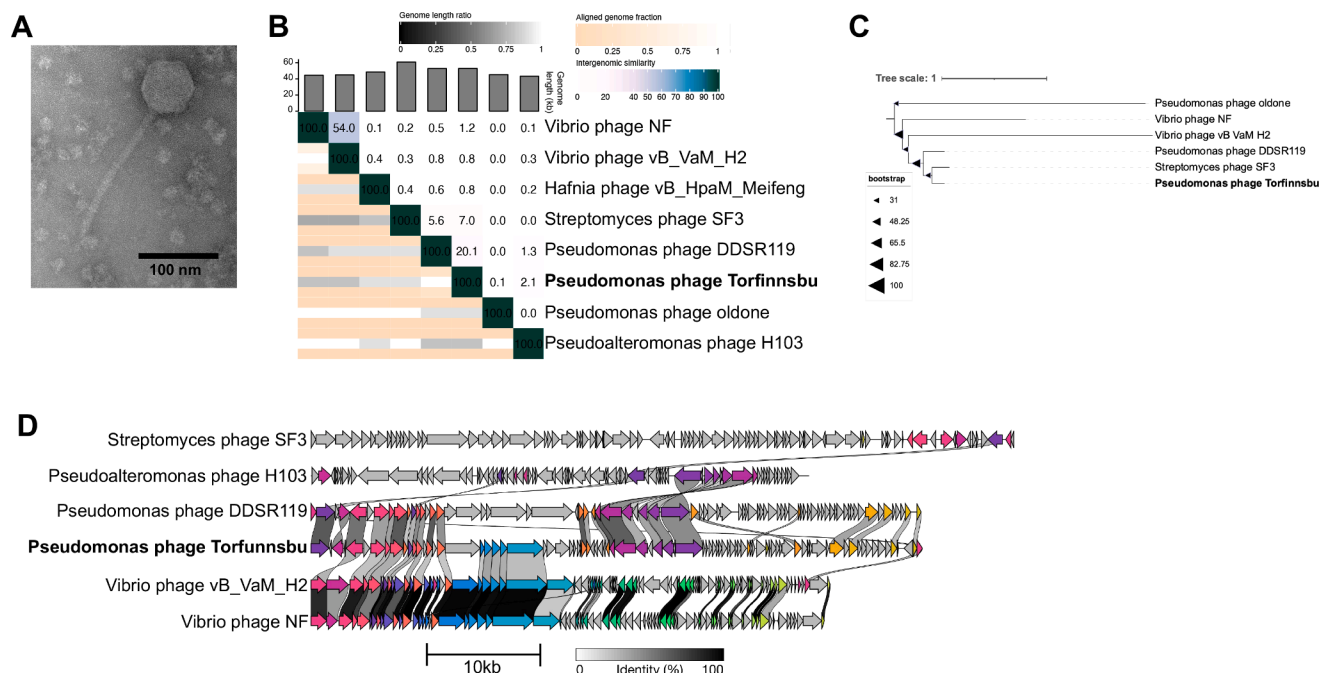


**Fig. 5.** Analysis of Pseudomonas phage Torfinnsbu. (A) TEM imaging of Pseudomonas phage Torfinnsbu. (B) Whole-genome nucleotide similarity of Torfinnsbu in comparison with select related phage genomes (VIRIDIC). (C) Bootstrapped maximum likelihood tree of large terminase subunit amino acid alignments with select related phages. (D) Clinker figure showing amino-acid similarities between protein-coding sequences. Protein clusters with > 30% sequence identity are coloured with the same colour.

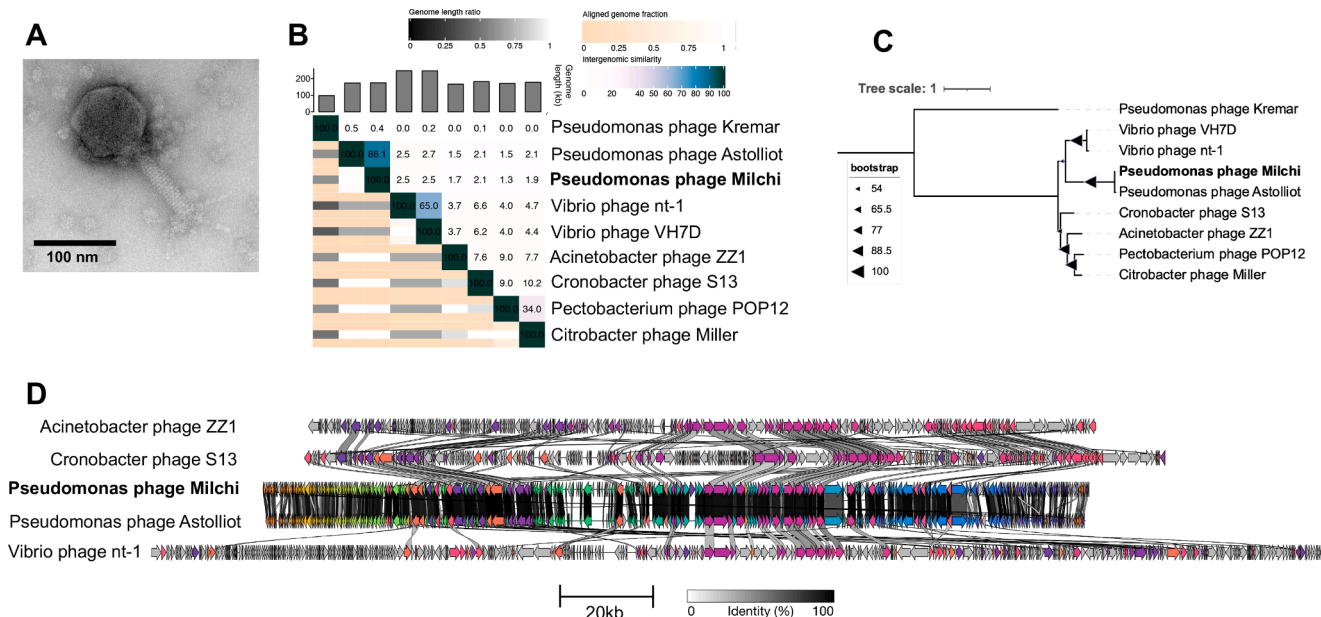


**Fig. 6.** Analysis of Pseudomonas phage Milchi. (A) TEM imaging of Pseudomonas phage Milchi. (B) Whole-genome nucleotide similarity of Milchi in comparison with select related phage genomes (VIRIDIC). (C) Bootstrapped maximum likelihood tree of large terminase subunit amino acid alignments with select related phages. (D) Clinker figure showing amino-acid similarities between protein-coding sequences. Protein clusters with > 30% sequence identity are coloured with the same colour.

Astolliot, with a whole genome nucleotide similarity of 86.1% (Fig. 6B), closely related TerL proteins (Fig. 6C) and highly conserved synteny and coding sequences (Fig. 6D). Based on this, Milchi should be placed in the same genus as Astolliot. On NCBI, Pseudomonas phage Astolliot has been placed into the genus *Otagovirus*, which has two ICTV-recognized species: Pseudomonas phage VCM and Pseudomonas phage phiPsa374 (Sisson et al., 2024). However, a VIRIDIC nucleotide comparison found that neither Milchi nor Astolliot has any significant nucleotide identity

(<0.2%) with members from either species. Using the commonly accepted 70% nucleotide identity threshold for phage genera, Milchi and Astolliot should therefore be reclassified and placed in a novel, separate genus as two new species.

### 3.7. Environmental distribution of similar phages

As all eight of these phage isolates were obtained from a different

environment (organic waste) than their bacterial hosts (wheat flag leaf), we were interested in which other environmental niches these phages inhabit. To investigate this, we combined environmental metadata from similar (>0.7 nucleotide similarity) phage isolates, metagenomically assembled phage contigs, and metagenomic SRAs. To search SRAs directly for similar phages, we used Branchwater (Luiz Irber, 2022) which samples a set of 21-mers from the query genome and compares them to sampled 21-mers from > 1,000,000 publicly available SRAs. We included hits with >70% kmer containment as an approximation of genus-level hits. Combining hits from isolates, metagenomic assemblies, and SRA, we analyzed the sample isolation environments (Supplementary Table 1).

No phages were found with genus-level similarity to *Pseudomonas* phages Boevelstad or Torfinnsbu in publically available isolate databases or metagenomes. This underlines both the need for phage isolations, the novelty of these two phages, and the sheer diversity of phage genomes worldwide; in > 1,000,000 metagenomic SRAs, no genus-level hits were found. In contrast, genus-level hits were found for *Pseudomonas* phages Milchi and Rembedalsseter, and *Erwinia* phages Vettismorki, Gravdalen, Hallingskeid, and Kaldavass (Fig. 7A). Interestingly, only the jumbo phages Hallingskeid and Kaldavass had metagenomic hits (IMGVR or Branchwater); all seven Hallingskeid hits were metagenomic, while 44/45 Kaldavass hits were metagenomic. This could be due to biases in phage isolation; for example, the crAssphage family is the most abundant in human gut microbiomes, yet the first crAss-like phage isolate was reported in 2018 (Shkoporov et al., 2018).

Although all phages were isolated from organic waste, genus-level phage hits were found in a greater variety of environments. Five of the phage isolates had hits from wastewater, illustrating why wastewater is so commonly used as a source for phage isolates. However, phage Kaldavass (45 hits) was dominated by hits to food and plant metagenomes. In each case where the food item was specified, it was a plant-based food, underlining how this phage appears to be conserved in a variety of plant microbiomes. Surprisingly, one Spanish spinach virome (SRR14611561 (Blanco-Picazo et al., 2022)) had 100% kmer containment at 100% identity to Kaldavass, indicating the presence of a (near) identical phage. To confirm this, we mapped the reads from this sample to Kaldavass and found only 227/366,556 bases in the entire genome (0.06%) had zero coverage (Fig. 7B). More broadly, the fact that a jumbo phage from organic waste in Denmark is near-identical to a phage from spinach in Spain and closely related to phages in American wastewater, speaks to how interconnected microbiomes are.

### 3.8. Phage-encoded anti-defense systems and DNA modifications

Next, we searched for anti-defense systems and DNA modifications in

the eight phage genomes. Using the dbAPIS (Yan et al., 2023) database of protein families derived from experimentally verified anti-defense systems, we conducted an HMM search for similar proteins in the phage genomes, followed by a BLASTP against the experimentally verified protein seed in each family (Table 2).

Only two of the phages had HMM hits to the dbAPIS database; *Pseudomonas* phages Rembedalsseter and Milchi. Interestingly, Milchi had 7/8 total dbAPIS hits from the nine phages, suggesting this phage may carry an especially high number of antidefense systems. However, these are very distant hits and should be treated with caution. Except for one good (89% coverage, 44% identity) Milchi hit to the anti-CBASS protein Acb1, BLASTP query coverage and identity were very low, and these proteins may not play any role in anti-defense. Conversely, we should not conclude that the other seven phages do not encode anti-defense systems. With dbAPIS only containing 41 experimentally verified seed proteins, we have only begun to scratch the surface of the phage repertoire of anti-defense systems.

In addition to explicit anti-defense systems, phages commonly use DNA modifications to avoid recognition by bacterial anti-phage defense systems such as RM and CRISPR-Cas9 (Hutinet et al., 2019; Kot et al., 2020; Olsen et al., 2023). We therefore searched for DNA modifications using Nanopore sequencing. By comparing the electrical signals generated from native phage DNA with that of WGA genome copies, we detected motifs associated with shifts in raw current signal levels, indicative of DNA modifications (Nielsen et al., 2023). These motifs, along with their predicted modification type, are shown in Table 3.

In contrast to the six other phages, native DNA from *Erwinia* phages Vettismorki and Gravdalen could not be sequenced with Nanopore technology. Although the WGA genomes could be sequenced and mapped, the native DNA reads were of so low quantity and quality that they could not be mapped back to their reference genomes. This is a known phenomenon when sequencing T-even phages with Nanopore technology, many of whom are known to be hypermodified with sugar molecules throughout the entire genome that greatly reduce read quality (shown for glucosyl-hydroxymethylcytosine (glc-hmC) in T4, and arabinose-hydroxymethylcytosine (ara-hmC) in RB69) (Nielsen et al., 2023). In this case, Vettismorki and Gravdalen have proteins with homology to both T4-encoded dCMP hydroxymethyltransferase (ESEGSTCX\_CDS\_0039 and ZRHYNTFE\_CDS\_0036) and dNMP kinase (ESEGSTCX\_CDS\_0157, ZRHYNTFE\_CDS\_0153) which produce hmC in T4 (Weigle and Raleigh, 2016a). However, the *Erwinia* phages have no homologs to the alpha and beta-glucosyltransferases required to produce glc-hmC in T4, or the proposed arabinosyltransferase found in RB69 (Thomas et al., 2018). They do however have close homologs to the RB69-encoded ORF53\_52C (ESEGSTCX\_CDS\_0044, ZRHYNTFE\_CDS\_0041) and ORF55C (ESEGSTCX\_CDS\_0046,

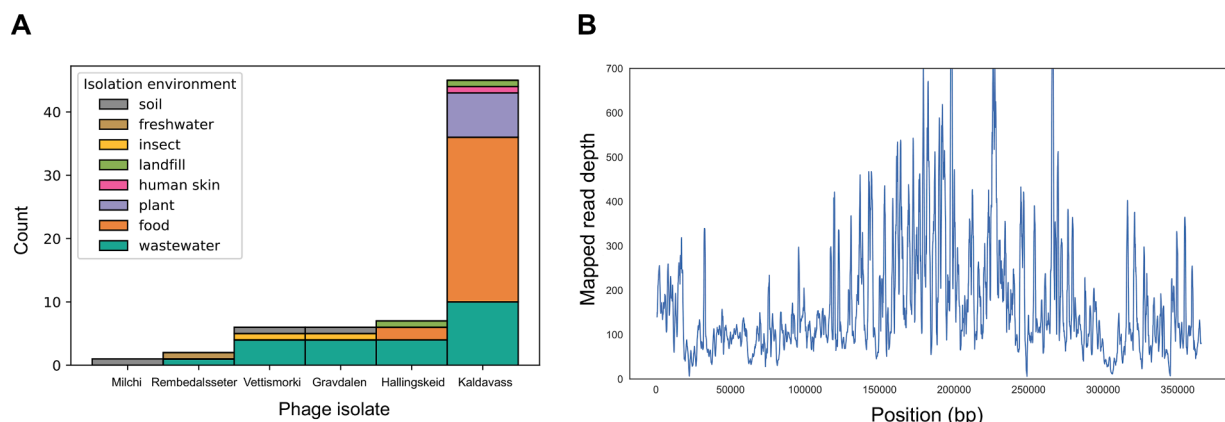


**Fig. 7.** (A) Breakdown of environments where similar phages were found. Environmental metadata was combined from similar (>70% nucleotide similarity) phage isolates and metagenomically assembled contigs, and SRAs with > 70% 21-mer containment, determined using Branchwater. (B) Read mapping from a Spanish spinach virome (SRR14611561) to the genome of phage Kaldavass, demonstrating near-complete genome coverage. Rolling average with window size = 1000 bp.



Table 2

HMM search for known anti-defense systems in the eight phage genomes using the dbAPIS database. Hits to APIS protein families were followed up with a BLASTP against the experimentally verified protein from each protein family. The bacterial defense system targeted by each verified anti-defense system is also shown.

Phage	Protein	APIS family hit	HMM e-value	Protein hit	BLASTP ID to hit	BLASTP query cover to hit	Target defence system
Rembedalsseter	EQXJUDKX_CDS_0022	AcrIF7	1.6E-03	AcrIF7	0.36	0.08	CRISPR
Milchi	HQEHHVWD_CDS_0033	APIS009	2.7E-04	RaI	0.19	0.41	RM
Milchi	HQEHHVWD_CDS_0047	APIS068	3.2E-03	Gad1	0.5	0.11	Gabija
Milchi	HQEHHVWD_CDS_0083	APIS055	1.1E-03	KlcA	0	0	RM
Milchi	HQEHHVWD_CDS_0125	APIS016	2.3E-28	Acb1	0.44	0.89	CBASS
Milchi	HQEHHVWD_CDS_0194	APIS023	5.3E-05	Gp5.9	0.3	0.3	RecBCD
Milchi	HQEHHVWD_CDS_0205	APIS060	7.5E-07	Apyc1	0	0	Pycsar
Milchi	HQEHHVWD_CDS_0209	APIS063	3.4E-06	ArdA	0.25	0.26	RM

Table 3

Summary of proposed DNA modifications, phage-encoded DNA methyltransferases, and modification motifs for each of the eight phages. Bold font indicates the modified base in the motif, while brackets indicate multiple variable bases. Known methylation motifs are indicated with \*. Ara-hmc is arabinose-hydroxymethylcytosine, a modification hypothesized based on protein homology with Escherichia phage RB69.

Phage	Predicted methyltransferases	Proposed modification type	Motifs
Vettismorki	0	ara-hmc	unknown
Gravdalen	0	ara-hmc	unknown
Hallingskeid	DMFGBAAK_CDS_0275	methylation	GATC*, CCWGG*
Kaldavass	DMFGBAAK_CDS_0623	methylation + unknown	GATC*, CCWGG*, TGCAT
	XGIBIPCR_CDS_0246		
	XGIBIPCR_CDS_0509		
Rembedalsseter	XGIBIPCR_CDS_0605	nicked DNA	WACTRTGAC
Boevelstad	IPGPQISR_CDS_0132	None	
Torfinnsbu	0	None	
Milchi	0	None	

ZRHYNTFE\_CDS\_0043) which are proposed to be involved in the synthesis of UDP-arabinose, a precursor to the ara-hmc (Thomas et al., 2018) modification. However, additional analysis is required to confirm the identity of the proposed hypermodification.

Of the eight phages investigated, two (Erwinia phages Hallingskeid and Kaldavass) displayed probable DNA modifications at two well-known methylation motifs; GATC and CC[AT]GG. These motifs are methylated in many bacteria and phages (modified by Dam and Dcm, respectively, in *E. coli*) (Marinus and Lobner-Olesen, 2009). We further analysed the modification data using motif-specific Tombo models for *E. coli* Dam and Dcm, confirming the presence of 6-methyladenine at GATC and 5-methylcytosine at CC[AT]GG. Erwinia phage Kaldavass was also modified at an additional motif (TGCAT). However, this motif is not present in the REBASE databases of restriction recognition systems and PacBio-identified methylation motifs (Roberts et al., 2005) and hence cannot be immediately identified. Both methylated phages also encoded DNA methyltransferases, although there was not a one-to-one correlation between the number of encoded methyltransferases and the number of modification motifs; Pseudomonas phage Boevelstad also encodes a predicted DNA methyltransferase, but did not have any detectable modification motifs. As the bacterial hosts also encode DNA methylases, it is also possible that phage DNA is methylated by host methylases rather than the phage-encoded methylases. Determining this would require the construction of methylase knockout mutants.

3.9. Pseudomonas phage Rembedalsseter has 13 single-stranded DNA breaks associated with a motif conserved in a large family of Pseudomonas phages

No DNA modification motifs were found in Pseudomonas phage Rembedalsseter. However, when investigating the native single-stranded sequencing depths, we were surprised to see that the

sequencing depth on the negative strand abruptly fell to zero (or near-zero) at 13 places throughout the genome (Fig. 8A). These coverage drops were not observed in the native positive strand, or in either strand of the WGA control. Analysing these 13 regions with MEME revealed a common motif present at all 13 sites: WACTRTGAC. This motif occurred precisely 13 times, all on the same strand, and perfectly correlating with the coverage drops.

A very similar motif (TACTRTGMC) was previously found to be associated with single-stranded DNA breaks (nicks) in the related Pseudomonas phage tf (Glukhov et al., 2012) (relationship shown in Fig. 3B-C). Single-stranded DNA breaks explain the Nanopore sequencing depth pattern; on one strand, no reads span the motif, and hence the coverage drops to zero at these motifs. Single-stranded breaks have also been observed in several other phages, including the distantly related Pseudomonas phages phiKf77 and phiKMV (Kulakov et al., 2009) (with a different motif), as well as the completely unrelated Escherichia phage T5 (Johnston et al., 1977). In all cases, the function of these nicks is unclear. Nick-less T5 mutants have been isolated, indicating the nicks are not necessary for T5 growth under laboratory conditions. Several explanations have been proposed, including the facilitation of DNA packaging (Glukhov et al., 2012) and gene expression (Kulakov et al., 2009).

To investigate how widespread Rembedalsseter's nick-associated motif (WACTRTGAC) is, we searched the INPHARED database for phages with similarity to Rembedalsseter and gathered the 250 phages with the highest aggregate tBLASTx score. We calculated the wGRR between each pair of these genomes, using this as an intergenomic distance metric (1 if each protein has an identical hit in the other genome, and 0 if none of the proteins are similar). We also counted the occurrences of the motif in each genome. Since the motif occurred only in one strand in Rembedalsseter, we calculated the net difference in number of motif occurrences between the two strands of each phage genome (Fig. 8B).

In Fig. 8B, Rembedalsseter clearly clusters with 60 related phages associated with a significantly higher net motif occurrence (9.0 within this cluster vs 0.7 outside this cluster). This cluster includes both Rembedalsseter and Pseudomonas phage tf. Statistically, this motif is also expected to occur by chance 0.7 times in a 45kbp genome, demonstrating that the motif is not enriched in phage genomes outside this cluster. This conserved motif occurrence is not simply a result of high genetic similarity; Rembedalsseter and tf share only minor nucleotide similarity (8% BLASTN coverage), but presumably reflects a conserved function of the nicks. Although it has previously been noted that similar nicked phages share motifs (Glukhov et al., 2012), this is the first systematic investigation into the distribution of nick-associated motifs in sequencing databases, revealing the extent of the motif conservation.

We also investigated how the motif was distributed within these 61 genomes. To enable comparisons between the diverse phages, we reoriented all phage genomes to start from the well-conserved *terL* gene, although this is a different start site than the physical end of the linear genome found in Rembedalsseter (correct orientation shown in Fig. 3D). Fig. 8C shows the nicks are not evenly spread but concentrated towards

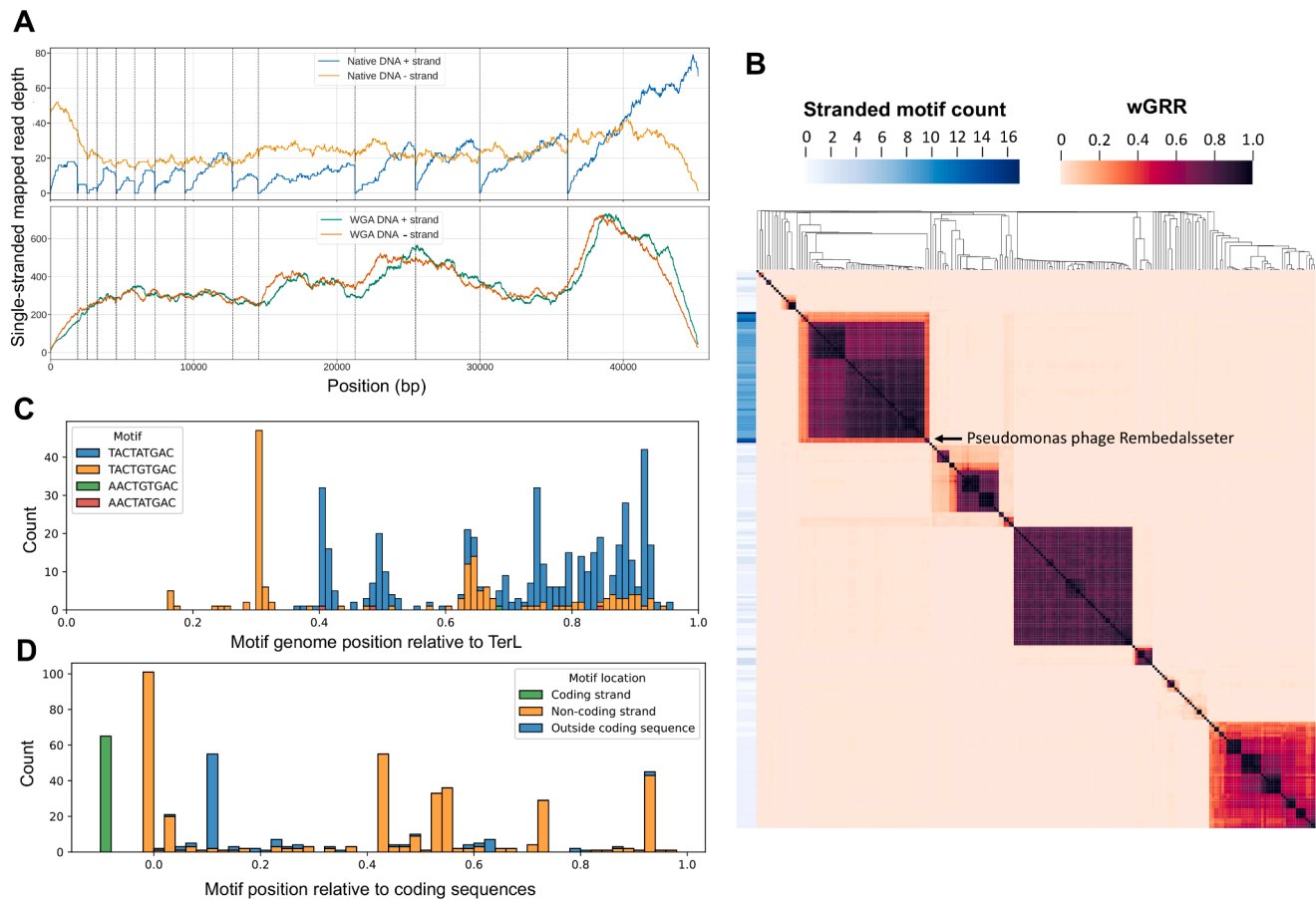


**Fig. 8.** Investigation of motifs associated with the single-stranded DNA breaks in *Pseudomonas* phage Rembedalsseter and comparison to related phages. **(A)** Single-stranded read-mapping depths of native and WGA DNA from Rembedalsseter. Dashed lines indicate WACTRTGAC motifs. **(B)** Heatmap of wGRR between Rembedalsseter and related phages with clustered rows and columns. Row labels indicate the difference in the number of WACTRTGAC motif occurrences between the two strands of each phage genome. *Pseudomonas* phage Rembedalsseter is indicated. **(C)** Position of motif locations relative to complete genome length in Rembedalsseter and the 60 related phages, with all genomes reoriented to start from *terL*. Bar colors indicate motif identity. **(D)** Motif locations relative to their position to the coding sequences they occur within (0 is the start of a coding sequence, and 1 is the end). Bar colors indicate motif strand relative to the coding sequence, and whether or not it occurs outside a coding sequence.

the right side of the *terL*-oriented genomes. In *Pseudomonas* phage *tf*, this part of the DNA molecule has been shown to be the first to attach to phage capsids, prompting the proposal that the nicks may play a role during packaging (Glukhov et al., 2012). Here, we show that this pattern of nick-associated motifs is conserved throughout this group of phages. We also found that only 4/542 motifs were AACTRTGAC, while the remaining were TACTRTGAC, with only three genomes containing AACTRTGAC motifs. However, Rembedalsseter has nicks associated with all four possible versions of the motif.

It has also been suggested that nicks may play a role in phage gene expression (Kulakov et al., 2009). To investigate this, we show the location of motifs relative to the coding sequences predicted by Phannotate (Fig. 8D). While 64 of the 542 motifs occur outside of coding sequences, the rest (88%) occur at least partly within coding sequences. This is nearly identical to the coding density of the host bacteria (89%), indicating coding sequences are not enriched in the motif. Although the motifs often occur at the beginning of coding sequences, they are also found throughout their length. They also occur mostly, though not exclusively, on the coding strand. This distribution throughout coding sequences and strands perhaps argues against a role in gene expression, although this data is merely descriptive and cannot exclude such a role.

We have known about nicked phage genomes for 50 years, yet their function remains enigmatic. Although a role in DNA packaging is plausible, it seems odd that nick-less mutants are viable if they aid such a crucial step in phage reproduction. A role for nicks in gene expression

also seems implausible given their distribution both throughout and outside of coding sequences. Perhaps they instead play a role in some non-essential processes, such as homologous recombination (where nicked DNA is an intermediate step) or protection against defence systems (where nicked DNA may protect against sequence recognition). However, all these hypotheses remain untested, and further studies are needed to explain the function of nicked phage genomes.

#### 4. Conclusion

In this study, we have isolated eight phages against *Pseudomonas* and *Erwinia* strains from the wheat phyllosphere, contributing to a growing collection of phage isolates targeting wheat phyllosphere bacteria. Based on phylogenetic analysis we propose the creation of four novel phage genera, with two of the phages having no genus-level hits even in metagenomic databases. Contrasting this diversity, other phages appear to be remarkably conserved; the jumbo phage genus *Mimavirus* appears to be widespread in plant microbiomes, with sequence reads from a near-identical phage to *Erwinia* phage Kaldavass found in a Spanish spinach microbiome.

Our results also underline the extent to which phages modify their DNA, finding methylation motifs in two jumbo phages and an unknown hypermodification in two *Winklervirus*. We also find a nick-associated motif from *Pseudomonas* phage Rembedalsseter to be conserved across a group of 61 phages, showing for the first time how ONT

sequencing can be used to investigate phage genome nicks. However, the function of these nicks remains unknown. More broadly, these results illustrate how much there is to learn from the isolation and characterization of new phage isolates.

## Funding

This research was supported and funded by the Novo Nordisk Foundation (grant number NNF19SA0059348).

## CRediT authorship contribution statement

**Peter Erdmann Dougherty:** Writing – review & editing, Writing – original draft, Visualization, Software, Investigation, Data curation, Conceptualization. **Maja Schmidt Pedersen:** Writing – review & editing, Investigation. **Laura Milena Forero-Junco:** Writing – review & editing, Visualization, Software, Investigation. **Alexander Byth Carstens:** Writing – review & editing, Investigation. **Jos M. Raaijmakers:** Writing – review & editing, Supervision. **Leise Riber:** Writing – review & editing, Supervision, Project administration, Investigation, Conceptualization. **Lars Hestbjerg Hansen:** Writing – review & editing, Supervision, Project administration, Conceptualization.

## Declaration of competing interest

The authors declare that they have no known competing financial interests or personal relationships that could have appeared to influence the work reported in this paper.

## Acknowledgments

The authors thank Natalie Allcock for her assistance with TEM imaging.

## Supplementary materials

Supplementary material associated with this article can be found, in the online version, at [doi:10.1016/j.virusres.2024.199524](https://doi.org/10.1016/j.virusres.2024.199524).

## Data availability

The datasets presented in this study can be found in online repositories. The names of the repository/repositories and accession number(s) can be found in the article.

## References

- Alanin, K.W.S., Olsen, N.S., Djurhuus, A.M., Carstens, A.B., Nielsen, T.K., Wagner, N., Lametsch, R., Bak, F., Hennessy, R.C., Nicolaisen, M.H., Kot, W., Hansen, L.H., 2023. Three novel phages isolated from organic waste represent three new genera. *Arch. Virol.* 168 (2).
- Bankovich, A., Nurk, S., Antipov, D., Gurevich, A.A., Dvorkin, M., Kulikov, A.S., Lesin, V. M., Nikolenko, S.I., Pham, S., Pribelski, A.D., Pyshkin, A.V., Sirotkin, A.V., Vyahhi, N., Tesler, G., Alekseyev, M.A., Pevzner, P.A., 2012. SPAdes: a new genome assembly algorithm and its applications to single-cell sequencing. *J. Comput. Biol.* 19 (5), 455–477.
- Blanco-Picazo, P., Gomez-Gomez, C., Tormo, M., Ramos-Barbero, M.D., Rodriguez-Rubio, L., Muniesa, M., 2022. Prevalence of bacterial genes in the phage fraction of food viromes. *Food Res. Int.* 156.
- Bouras, G., Nepal, R., Houtak, G., Psaltis, A.J., Wormald, P.J., Vreugde, S., 2023. PharoKka: a fast scalable bacteriophage annotation tool. *Bioinformatics* 39 (1).
- Buttner, C., Hendrix, H., Oliveira, H., Casey, A., Neve, H., McAuliffe, O., Ross, R.P., Hill, C., Noben, J.P., O'Mahony, J., Lavigne, R., Coffey, A., 2017. Things are getting hairy: enterobacteria bacteriophage vB\_PcaM\_CBB. *Front. Microbiol.* 8, 44.
- Camargo, A.P., Roux, S., Schulz, F., Babinski, M., Xu, Y., Hu, B., Chain, P.S.G., Nayfach, S., Kyrpides, N.C., 2024. Identification of mobile genetic elements with geNomad. *Nat. Biotechnol.* 42, 1303–1312.
- Ceyssens, P.J., Hertveldt, K., Ackermann, H.W., Noben, J.P., Demeke, M., Volckaert, G., Lavigne, R., 2008. The intron-containing genome of the lytic *Pseudomonas* phage LUZ24 resembles the temperate phage PaP3. *Virology* 377 (2), 233–238.
- Chen, B., Akusobi, C., Fang, X., Salmund, G.P.C., 2017. Environmental T4-family bacteriophages evolve to escape abortive infection via multiple routes in a bacterial host employing "Altruistic suicide" through type III toxin-antitoxin systems. *Front. Microbiol.* 8, 1006.
- Clokie, M.R., Millard, A.D., Letarov, A.V., Heaphy, S., 2011. Phages in nature. *Bacteriophage* 1 (1), 31–45.
- Cook, R., Brown, N., Redgwell, T., Rihtman, B., Barnes, M., Clokie, M., Stekel, D.J., Hobman, J., Jones, M.A., Millard, A., 2021. INfrastructure for a PHAge REference database: identification of large-scale biases in the current collection of cultured phage genomes. *Phage (New. Rochelle)* 2 (4), 214–223.
- Djurhuus, A.M., Carstens, A.B., Neve, H., Kot, W., Hansen, L.H., 2020. Two new phages with odd growth patterns expand the diversity of phages infecting soft rot. *Phage-Ther. Appl. Res.* 1 (4), 251–259.
- Dougherty, P.E., Nielsen, T.K., Riber, L., Lading, H.H., Forero-Junco, L.M., Kot, W., Raaijmakers, J.M., Hansen, L.H., 2023. Widespread and largely unknown prophage activity, diversity, and function in two genera of wheat phyllosphere bacteria. *ISME J.*
- Duan, N., Hand, E., Pheko, M., Sharma, S., Emiola, A., 2024. Structure-guided discovery of anti-CRISPR and anti-phage defense proteins. *Nat. Commun.* 15 (1).
- Edgar, R.C., 2004. MUSCLE: multiple sequence alignment with high accuracy and high throughput. *Nucl. Acids Res.* 32 (5), 1792–1797.
- Eller, M.R., Vidigal, P.M., Salgado, R.L., Alves, M.P., Dias, R.S., da Silva, C.C., de Carvalho, A.F., Kropinski, A., De Paula, S.O., 2014. UFV-P2 as a member of the LUZ24likevirus genus: a new overview on comparative functional genome analyses of the LUZ24-like phages. *BMC Genom.* 15, 7.
- Felix Krueger, F.J., P. Ewels, E. Afyounian, M. Weinstein, B. Schuster-Boeckler, G. Hulsemans, Sclamons, 2021. FelixKrueger/TrimGalore v0.6.6.
- Forero-Junco, L.M., Alanin, K.W.S., Djurhuus, A.M., Kot, W., Gobbi, A., Hansen, L.H., 2022. Bacteriophages roam the wheat phyllosphere. *Viruses-Basel* 14 (2), 244.
- Frampton, R.A., Pitman, A.R., Fineran, P.C., 2012. Advances in bacteriophage-mediated control of plant pathogens. *Int. J. Microbiol.* 2012, 326452.
- Georjon, H., Bernheim, A., 2023. The highly diverse antiphage defence systems of bacteria. *Nat. Rev. Microbiol.* 21 (10), 686–700.
- Gilchrist, C.L.M., Chooi, Y.H., 2021. Clinker & clustermap.js: automatic generation of gene cluster comparison figures. *Bioinformatics* 37 (16), 2473–2475.
- Glukhov, A.S., Krutina, A.I., Shlyapnikov, M.G., Severinov, K., Lavysh, D., Kochetkov, V.V., McGrath, J.W., de Leeuw, C., Shaburova, O.V., Krylov, V.N., Akulenko, N.V., Kulakov, L.A., 2012. Genomic analysis of *Pseudomonas putida* phage if with localized single-strand DNA interruptions. *PLoS One* 7 (12), e51163.
- Herpell, J.B., Alicovic, A., Diallo, B., Schindler, F., Weckwerth, W., 2023. Phyllosphere symbiont promotes plant growth through ACC deaminase production. *ISME J.* 17 (8), 1267–1277.
- Hockenberry, A.J., Wilke, C.O., 2021. BACPHILIP: predicting bacteriophage lifestyle from conserved protein domains. *PeerJ* 9, e11396.
- Howard-Varona, C., Hargreaves, K.R., Abedon, S.T., Sullivan, M.B., 2017. Lysogeny in nature: mechanisms, impact and ecology of temperate phages. *ISME J.* 11 (7), 1511–1520.
- Hutinet, G., Kot, W., Cui, L., Hillebrand, R., Balamkundu, S., Gnanakalai, S., Neelakandan, R., Carstens, A.B., Lui, C.F., Tremblay, D., Jacobs-Sera, D., Sassanfar, M., Lee, Y.J., Weigele, P., Moineau, S., Hatfull, G.F., Dedon, P.C., Hansen, L.H., de Crécy-Lagard, V., 2019. 7-Deazaguanine modifications protect phage DNA from host restriction systems. *Nat. Commun.* 10.
- Jo, D., Kim, H., Lee, Y., Kim, J., Ryu, S., 2023. Characterization and genomic study of EJP2, a novel jumbo phage targeting antimicrobial resistant *Escherichia coli*. *Front. Microbiol.* 14, 1194435.
- Johnston, J.V., Nichols, B.P., Donelson, J.E., 1977. Distribution of minor nicks in bacteriophage-T5 DNA. *J. Virol.* 22 (2), 510–519.
- Jorgensen, J.B., Djurhuus, A.M., Carstens, A.B., Kot, W., Neve, H., Morris, C.E., Hansen, L.H., 2020. Presentation of three novel tailed phages targeting multiple strains of. *Phage-Ther. Appl. Res.* 1 (4), 245–250.
- Junco, L.M.F., 2024. TOMBO HP Workflow. Github.
- Knezevic, P., Petrovic Fabijan, A., Gavric, D., Pejic, J., Doffkay, Z., Rakhely, G., 2021. Phages from genus Bruynoghevirus and phage therapy: *Pseudomonas* phage delta case. *Viruses* 13 (10), 1965.
- Kot, W., Olsen, N.S., Nielsen, T.K., Hutinet, G., de Crécy-Lagard, V., Cui, L., Dedon, P.C., Carstens, A.B., Moineau, S., Swairjo, M.A., Hansen, L.H., 2020. Detection of preQ deazaguanine modifications in bacteriophage CAjan DNA using Nanopore sequencing reveals same hypermodification at two distinct DNA motifs. *Nucl. Acids Res.* 48 (18), 10383–10396.
- Kulakov, L.A., Ksenzenko, V.N., Shlyapnikov, M.G., Kochetkov, V.V., Del Casale, A., Allen, C.C.R., Larkin, M.J., Ceyssens, P.J., Lavigne, R., 2009. Genomes of "phiKMV-like viruses" of contain localized single-strand interruptions. *Virology* 391 (1), 1–4.
- Iyer, L.M., Anantharaman, V., Krishnan, A., Burroughs, A.M., Aravind, L., 2021. Jumbo phages: a comparative genomic overview of core functions and adaptations for biological conflicts. *Viruses* 13 (1), 63.
- Letunic, I., Bork, P., 2021. Interactive Tree Of Life (iTOL) v5: an online tool for phylogenetic tree display and annotation. *Nucl. Acids Res.* 49 (W1), W293–W296.
- Li, H., 2018. Minimap2: pairwise alignment for nucleotide sequences. *Bioinformatics* 34 (18), 3094–3100.
- Li, H., Durbin, R., 2009. Fast and accurate short read alignment with Burrows-Wheeler transform. *Bioinformatics* 25 (14), 1754–1760.
- Li, L., Xin, X.Z., Zhao, J., Yang, A.X., Wu, S.L., Zhang, H.L., Yu, S.S., 2023. Remote sensing monitoring and assessment of global vegetation status and changes during 2016–2020. *Sensors-Basel* 23 (20), 8452.
- Liu, X.Y., Matsumoto, H., Lv, T.X., Zhan, C.F., Fang, H.D., Pan, Q.Q., Xu, H.R., Fan, X.Y., Chui, T.Y., Chen, S.L., Qiao, K., Ma, Y.N., Sun, L., Wang, Q.W., Wang, M.C., 2023. Phyllosphere microbiome induces host metabolic defence against rice false-smut disease. *Nat. Microbiol.* 8 (8), 1419. →.



- Luiz Irber, N.T.P.-W., C. Titus Brown, 2022. Sourmash branchwater enables lightweight petabyte-scale sequence search. *bioRxiv*.
- Marinus, M.G., Lobner-Olesen, A., 2009. DNA methylation. *EcoSal. Plus* 6 (1).
- Minh, B.Q., Schmidt, H.A., Chernomor, O., Schrempf, D., Woodhams, M.D., von Haeseler, A., Lanfear, R., 2020. IQ-TREE 2: new models and efficient methods for phylogenetic inference in the genomic era. *Mol. Biol. Evol.* 37 (5), 1530–1534.
- Moraru, C., Varsani, A., Kropinski, A.M., 2020. VIRIDIC-a novel tool to calculate the intergenomic similarities of prokaryote-infecting viruses. *Viruses-Basel* 12 (11).
- Morella, N.M., Gomez, A.L., Wang, G., Leung, M.S., Koskella, B., 2018. The impact of bacteriophages on phyllosphere bacterial abundance and composition. *Mol. Ecol.* 27 (8), 2025–2038.
- Nielsen, T.K., Forero-Junco, L.M., Kot, W., Moineau, S., Hansen, L.H., Riber, L., 2023. Detection of nucleotide modifications in bacteria and bacteriophages: strengths and limitations of current technologies and software. *Mol. Ecol.* 32 (6), 1236–1247.
- Olsen, N.S., Nielsen, T.K., Cui, L., Dedon, P., Neve, H., Hansen, L.H., Kot, W., 2023. A novel Queuovirinae lineage of *Pseudomonas aeruginosa* phages encode dPreQ DNA modifications with a single GA motif that provide restriction and CRISPR Cas9 protection in vitro. *Nucl. Acids Res.* 51 (16), 8663–8676.
- Pfeifer, E., de Sousa, J.A.M., Touchon, M., Rocha, E.P.C., 2021. Bacteria have numerous distinctive groups of phage-plasmids with conserved phage and variable plasmid gene repertoires. *Nucl. Acids Res.* 49 (5), 2655–2673.
- Pfeilmeier, S., Caly, D.L., Malone, J.G., 2016. Bacterial pathogenesis of plants: future challenges from a microbial perspective: challenges in bacterial molecular plant pathology. *Mol. Plant Pathol.* 17 (8), 1298–1313.
- Prichard, A., Lee, J.A., Laughlin, T.G., Lee, A.M., Thomas, K.P., Sy, A.E., Spencer, T., Asavavimol, A., Cafferata, A., Cameron, M., Chiu, N., Davydov, D., Desai, I., Diaz, G., Guereca, M., Hearst, K., Huang, L.Y., Jacobs, E., Johnson, A., Kahn, S., Koch, R., Martinez, A., Norquist, M., Pau, T., Prasad, G., Saam, K., Sandhu, M., Sarabia, A.J., Schumaker, S., Sonin, A., Uyeno, A., Zhao, A.L.S., Corbett, K.D., Pogliano, K., Meyer, J., Grose, J.H., Villa, E., Dutton, R., Pogliano, J., 2023. Identifying the core genome of the nucleus-forming bacteriophage family and characterization of phage RAY. *Cell Rep.* 42 (5), 112432.
- Rasmussen, T.S., Mentzel, C.M.J., Kot, W., Castro-Mejia, J.L., Zuffa, S., Swann, J.R., Hansen, L.H., Vogensen, F.K., Hansen, A.K., Nielsen, D.S., 2020. Faecal virome transplantation decreases symptoms of type 2 diabetes and obesity in a murine model. *Gut* 69 (12), 2122–2130.
- Riber, L., Carstens, A.B., Dougherty, P.E., Roy, C., Willenbücher, K., Hille, F., Franz, C.M. A.P., Hansen, L.H., 2023. Pheno- and genotyping of three novel bacteriophage genera that target a wheat phyllosphere genus. *Microorganisms* 7, 1831.
- Roberts, R.J., Vincze, T., Posfai, J., Macelis, D., 2005. REBASE–restriction enzymes and DNA methyltransferases. *Nucl. Acids Res.* 33 (Database issue), D230–D232.
- Shen, W., Le, S., Li, Y., Hu, F.Q., 2016. SeqKit: a cross-platform and ultrafast toolkit for FASTA/Q file manipulation. *PLoS One* 11 (10).
- Shkoporov, A.N., Khokhlova, E.V., Fitzgerald, C.B., Stockdale, S.R., Draper, L.A., Ross, R. P., Hill, C., 2018.  $\Phi$ CrAss001 represents the most abundant bacteriophage family in the human gut and infects. *Nat. Commun.* 9, 4781.
- Simoliunas, E., Kaliniene, L., Truncaite, L., Zajanckauskaite, A., Staniulis, J., Kaupinis, A., Ger, M., Valius, M., Meskys, R., 2013. Klebsiella phage vB\_KleM-RaK2 - a giant singleton virus of the family Myoviridae. *PLoS One* 8 (4), e60717.
- Simón, D., Cristina, J., Musto, H., 2021. Nucleotide composition and codon usage across viruses and their respective hosts. *Front. Microbiol.* 12, 646300.
- Sisson, H.M., Fagerlund, R.D., Jackson, S.A., Briers, Y., Warring, S.L., Fineran, P.C., 2024. Antibacterial synergy between a phage endolysin and citric acid against the Gram-negative kiwifruit pathogen *Pseudomonas syringae* pv. *actinidiae*. *Appl. Environ. Microbiol.* 90 (3), e0184623.
- Sohrabi, R., Paasch, B.C., Liber, J.A., He, S.Y., 2023. Phyllosphere microbiome. *Annu Rev. Plant Biol.* 74, 539–568.
- Storey, N., Rabiey, M., Neuman, B.W., Jackson, R.W., Mulley, G., 2020. Genomic characterisation of mushroom pathogenic pseudomonads and their interaction with bacteriophages. *Viruses* 12 (11), 1286.
- Sun, C.Q., Chen, J.C., Jin, M.L., Zhao, X.Y., Li, Y., Dong, Y.Q., Gao, N., Liu, Z., Bork, P., Zhao, X.M., Chen, W.H., 2023. Long-read sequencing reveals extensive DNA methylations in human gut phagenome contributed by prevalently phage-encoded methyltransferases. *Adv. Sci.* 10 (25).
- Tan, Y., Zhang, K., Rao, X., Jin, X., Huang, J., Zhu, J., Chen, Z., Hu, X., Shen, X., Wang, L., Hu, F., 2007. Whole genome sequencing of a novel temperate bacteriophage of *P. aeruginosa*: evidence of tRNA gene mediating integration of the phage genome into the host bacterial chromosome. *Cell Microbiol.* 9 (2), 479–491.
- Thomas, J.A., Orwenyo, J., Wang, L.X., Black, L.W., 2018. The odd “RB” phage-identification of arabinosylation as a new epigenetic modification of DNA in T4-like phage RB69. *Viruses* 10 (6), 313.
- Turner, D., Kropinski, A.M., Adriaenssens, E.M., 2021. A roadmap for genome-based phage taxonomy. *Viruses-Basel* 13 (3), 506.
- Villicaña, C., Rubí-Rangel, L.M., Amarillas, L., Lightbourn-Rojas, L., Carrillo-Fasio, J., León-Félix, J., 2024. Isolation and characterization of two novel genera of jumbo bacteriophages infecting isolated from agricultural regions in Mexico. *Antibiotics-Basel* 13 (7), 651.
- Weigle, P., Raleigh, E.A., 2016a. Biosynthesis and function of modified bases in bacteria and their viruses. *Chem. Rev.* 116 (20), 12655–12687.
- Weigle, P., Raleigh, E.A., 2016b. Biosynthesis and function of modified bases in bacteria and their viruses. *Chem. Rev.* 116 (20), 12655–12687.
- Yan, Y.C., Zheng, J.F., Zhang, X.P., Yin, Y.B., 2023. dbAPIS: a database of anti-prokaryotic immune system genes. *Nucl. Acids Res.* 27;52 (D1), D419–D425.